

Neural parabolic wave equation for refractivity estimation

Mikhail S. Lytaev^[0000-0001-7082-4716]

St. Petersburg Federal Research Center of the Russian Academy of Sciences,
14-th Linia, V.I., No. 39, Saint Petersburg 199178, Russia

Abstract The inverse problem of estimating the refractive index in a waveguide based on wave field measurement data is studied. A differentiable finite-difference scheme for the parabolic wave equation is constructed. The desired function of spatial coordinates, corresponding to the refractive index, is represented as a deep neural network. Optimization problem with respect to unknown refractive index function is formulated and solved. Automatic differentiation of the numerical scheme is used for efficient gradient computation. Numerical examples confirm that the proposed method outperforms the existing approaches to solving underwater and tropospheric tomography problems.

Keywords: inverse problem · physics informed machine learning · ill-posed problem · radiowave propagation · underwater acoustics · JAX

1 Introduction

Refraction has a decisive impact on wave propagation in large unbounded domains such as troposphere [14] or underwater environments [9]. Tropospheric refractive index may form waveguides that transmit radio signals for hundreds of kilometers near the Earth's surface. Similarly, acoustic signals propagate in the sea for hundreds and thousands of kilometers under the influence of the underwater sound speed profile. Despite this, reliable methods for real-time measurement or estimation of atmospheric refractivity parameters [21,20] or oceanic parameters [19] have not yet been developed. The size of the region is too large for realtime direct measurements, so inversion based on indirect measurements seems the most promising. Mathematically, the complexity of the inversion problem lies in its nonlinearity and ill-posedness in the sense of Hadamard [6].

From the point of view of classical theory, nonlinear ill-posed problems are rather hopeless for a reliable solution [25]. Even if a solution can be found, it takes hours or days of extensive computations, i.e., the results become irrelevant [7]. On the other hand, problems solved by modern machine learning (ML), including scientific ML [24], are also ill-posed but are often successfully and quickly solved by modern neural network architectures and optimization methods. This suggests the use of ML tools in the problem of refractive index inversion.

Physics-informed machine learning models often suffer from a lack of interpretability. The ML approach usually relies on data rather than laws and

equations. However, high-quality data in physical problems is a rarity. A quite successful attempt to overcome this issue is the method of physics-informed neural networks (PINN) [15]. PINN allows incorporating physical laws into the objective function, thereby increasing the accuracy and interpretability of the results. PINN is suitable for solving both direct and inverse problems. One of disadvantages of PINN is that it does not take into account the specifics of numerical modeling of the processes it works with. In particular, this is evident in wave propagation modeling in waveguides, where the main difficulty lies in the numerical solution, as the computational domain is very large.

To account for the specifics of numerical implementation, one can substitute numerical scheme for the original physical laws into the objective function. This allows taking into account numerical features but requires differentiating the numerical schemes. Differentiable numerical schemes have already shown their effectiveness in problems of hydrodynamics [3,1], mechanics, thermodynamics [26], and underwater acoustics [17].

In this work, for the first time, the unknown profile is sought in the form of a deep neural network. The parabolic equation method is used as the numerical scheme for the corresponding forward problem, which is equally well suited for solving underwater acoustics problems [5] and tropospheric radio wave propagation [14]. This explains the title of the present paper. The idea of this research is largely inspired by the works [4,12] on neural differential equations, which proposed building models that simultaneously include differential equations and neural networks. This approach allows taking into account wave dynamics using strict wave equations, while poorly interpretable features such as refractive index inhomogeneities are modeled and estimated using neural networks.

2 Mathematical formulation of the problem

This section discloses the relationship between the direct and inverse wave propagation problems.

2.1 Direct problem and its solution

The wave process is modeled by the two-dimensional Helmholtz equation [14]

$$\frac{\partial^2 \psi}{\partial x^2} + \frac{\partial^2 \psi}{\partial z^2} + k^2 n^2(z) \psi = 0, \quad (1)$$

where $\psi(x, z)$ is the complex-valued two-dimensional distribution of the wave field, $n(z)$ is the refractive index of the medium, $k = 2\pi/\lambda$ is the wavenumber, λ is the wavelength. Depending on the specifics of a particular problem, function ψ satisfies certain initial and boundary conditions.

It is assumed that the length (along the x coordinate) of the computational domain significantly exceeds the height (along the z coordinate), i.e., propagation occurs in an elongated waveguide. Under these conditions, refractive index $n(z)$ has a decisive influence on the long range wave propagation.

The problem of finding wave field $\psi(x, z)$ given the refractive index $n(z)$, initial and boundary conditions is called the direct one. It is generally well-posed, i.e., has a unique solution. There are several methods for solving the direct problem for the Helmholtz equation, but the parabolic equation method and its generalization, called the one-way Helmholtz equation, best suit the specifics of the problem being solved [14,5].

Ignoring backscattering, equation (1) can be formally rewritten in the one-way form [18,8]

$$\frac{\partial \psi}{\partial x} = i \sqrt{\frac{\partial^2}{\partial z^2} + k^2 n^2(z)} \psi.$$

Using the operator exponential, the step-by-step solution can be written as

$$u(x + \Delta x, z) = \mathcal{P}(n) u(x, z),$$

$$u(x, z) = \psi(x, z) \exp(-ikx),$$

$$\mathcal{P}(n) u = \exp \left(ik \Delta x \left(\sqrt{\frac{1}{k^2} \frac{\partial^2}{\partial z^2} + n^2(z)} - 1 \right) \right) u. \quad (2)$$

Thus, the direct problem reduces to the numerical approximation of the operator exponential (2). In this work, we use the finite-difference rational approximation method [18]. Within the present research, it is essential that the numerical approximation of (2) is implemented in a finite number of sequential steps. Indeed, as it is shown in [18], the entire step-by-step solution process essentially consists of sequentially solving one-dimensional differential equations of the form

$$\left[1 + b_i \left(\frac{1}{k^2} \frac{\partial^2}{\partial z^2} + n^2(z) - 1 \right) \right] u_{i+1}(z) = \left[1 + a_i \left(\frac{1}{k^2} \frac{\partial^2}{\partial z^2} + n^2(z) - 1 \right) \right] u_i(z). \quad (3)$$

After discretization along the z variable, this equation reduces to a tridiagonal system of linear algebraic equations, which is solved in linear time using the tridiagonal matrix algorithm.

2.2 Inverse problem formulation

In the inverse problem, the refractive index $n(z)$ is unknown. However, the values of the wave field ψ at some points in space (x_i, z_i) , $i = 1..N$ are known. We denote the vector of these measurements as \mathbf{v} .

The complexity of the inverse problem lies in its ill-posedness in the sense of Hadamard. It is unknown whether a solution exists and whether it is unique. Indeed, there may be too few measurements, or they may be too noisy.

Let $\mathcal{G}(n)$ denote operator that solves the direct problem at points (x_i, z_i) , $i = 1..N$ for the refractive index n . Then the inverse operator $\mathcal{G}^{-1}(\mathbf{v})$, mapping the wave field measurement data to the refractive index, will be the solution to the inverse problem. We express the inverse operator $\mathcal{G}^{-1}(\mathbf{v})$ in terms of $\mathcal{G}(n)$ and the functional minimization problem

$$\mathcal{G}^{-1}(\mathbf{v}) = \arg \min_n \text{Loss}(\mathcal{G}(n), \mathbf{v}), \quad (4)$$

where

$$\text{Loss}(\mathcal{G}(n), \mathbf{v}) = \|\mathcal{G}(n) - \mathbf{v}\|^2 + \gamma \left\| \frac{\partial n}{\partial z} \right\|^2. \quad (5)$$

Indeed, the inverse problem can be viewed as finding such a refractive index $n(z)$ that minimizes the difference between the measured field and the field predicted by the direct model. This is what the first term of the objective functional (5) is responsible for. The second term is responsible for regularization [25]. It eliminates strongly oscillating solutions that formally minimize the functional but have no physical meaning.

Note that this functional does not have any special properties such as convexity or linearity, so its minimization is a highly non-trivial problem.

3 Refractive index inversion

As we saw in the previous section, the inverse problem of refractive index inversion is formulated as a minimization problem of a functional that includes solution to the direct problem. The space of functions is infinite-dimensional, so the first thing to do for the numerical minimization of functional (5) is to determine the search space. Usually, vertical refractive index profile is sought in the form of a finite set of values on a given grid [27,10]. In this work, it is proposed to estimate the refractive index in the form of a multilayer perceptron with one input (height z), one output (real-valued refractive index), and several hidden layers. Thus, the minimization problem reduces to finding the optimal value of a finite number of neural network weights (θ).

There are essentially two large classes of solution methods: stochastic global methods [23] and local methods [7] based on gradient descent. Global methods are convenient because they do not require any additional information about the minimized functional. A black box that outputs the value of the functional at any point in the search space is sufficient. Unfortunately, even with the most successful parameterization, the number of parameters to be determined is one or several tens. Global methods converge extremely slowly, given that it is not any but a specific global minimum that is being sought.

Local optimization methods, which use the gradient of the minimized function with respect to the unknown parameters, are significantly more efficient. Following the gradient direction significantly increases the convergence rate, at least to a local minimum. This is the basis of all existing methods for training

neural networks. They are successfully trained, although may have millions of unknown parameters. The difficulty here is precisely the requirement of having a gradient. The use of the finite-difference approach is inefficient due to the catastrophic cancellation problem [2].

For the neural networks training, the automatic differentiation method [2] is used. Its essence lies in representing the network as a computational acyclic graph consisting of elementary operations. Although there may be quite a few of them, sequential automatic application of differentiation rules allows efficient analytical computation of the gradient.

For a long time, this approach was limited to neural networks. A certain revolution here was made by the JAX framework [22], which allowed representing functions and algorithms of a very arbitrary form as a computational graph and, accordingly, automatically differentiating them. At the same time, the programming interface, as much as possible, repeats the widely used numerical modeling libraries numpy and scipy.

Functional (5) is significantly more complex than those usually used in machine learning, as it contains the operator of the direct problem solution. One can, following the adjoint equation method [10,19], try to differentiate operator \mathcal{G} analytically. This leads to the need to derive and numerically solve a new adjoint equation. There is low flexibility in choosing the representation of the function to be determined within the adjoint method. A much more efficient approach seems to be representing the numerical implementation of the operator \mathcal{G} as a computational graph using the JAX framework.

Note that numerical scheme (3) consists of a known sequence of elementary operations. Therefore, it can be represented as a computational graph. The method is implemented within the PyWaveProp library and is freely available [16].

The proposed solution is schematically presented in Fig. 1. $n_\theta(z)$ is sought in the form of a multilayer perceptron with a finite unknown set of real parameters θ (the nodes of the network). At the same time, $n_\theta(z)$ is an argument of the operator \mathcal{G} , the numerical implementation of which is an automatically differentiable computational graph with respect to θ . In addition, the vector of field measurements \mathbf{v} is fed as input. This configuration allows automatic computation of the required gradient $\nabla_\theta Loss$.

The resulting gradient computation algorithm is used by one or another local optimization algorithm to search for the optimal parameters θ . Following most works on deep learning, including PINN, in this research we use the Adam method [13] for optimization.

4 Numerical results and discussion

The general scheme of computational experiments is based on the inversion of synthetic data. A typical refractive index profile is selected. Using the direct problem solution method, the value at points corresponding to the location of the receivers is computed. Random noise is added to these values. The resulting

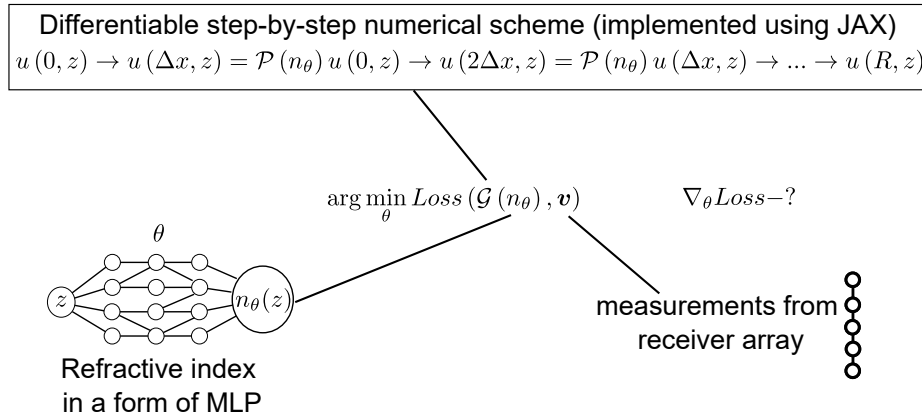


Figure 1. Schematic description of the inversion algorithm.

noisy synthetic measurements are fed to the inversion algorithm, which estimates the refractive index. At the end, the original and inverted profiles are compared.

4.1 Tropospheric refractive index estimation

The schematic description of the tropospheric refractive index inversion problem is shown in Fig. 2. A source with known parameters emits a radio signal received by a vertical array of receivers. As the signal propagates between the source and the receiver, it is influenced by the inhomogeneities of the tropospheric refractive index. By analyzing the received signal, it is required to determine the tropospheric refractive index.

In this work, only a monochromatic source emitting at a frequency of 3 GHz is considered. The receiver array is located at a distance of 5 km from the source. The array consists of 17 point receivers uniformly located at heights of 5-170 m. The signal-to-noise ratio at the receivers is assumed to be 30 dB.

Unless otherwise specified, refractive index profile is sought in the form of a multilayer perceptron with 4 hidden layers of width 50. The Adam method with a learning rate of 0.05 and regularization parameter $\gamma = 10^{-3}$ is used.

Let us check the fundamental possibility of inversion for typical tropospheric waveguides [14]: surface duct, surface-based duct, and elevated duct. It can be seen from Fig. 3 that the proposed method successfully inverted four different typical tropospheric refractive index profiles. At the same time, the method does not require any prior information about the profile distribution.

Fig. 4 depicts the two-dimensional distribution of the electromagnetic field computed for the original and inverted profiles. The influence of the waveguide effects on propagation near the Earth's surface is clearly observable. The elevated waveguide focuses the field near the Earth's surface (up to 100 m), with zones of strong signal and shadow alternating with each other. It can be seen that the patterns for the original and inverted profiles differ slightly. For clarity, Fig. 5

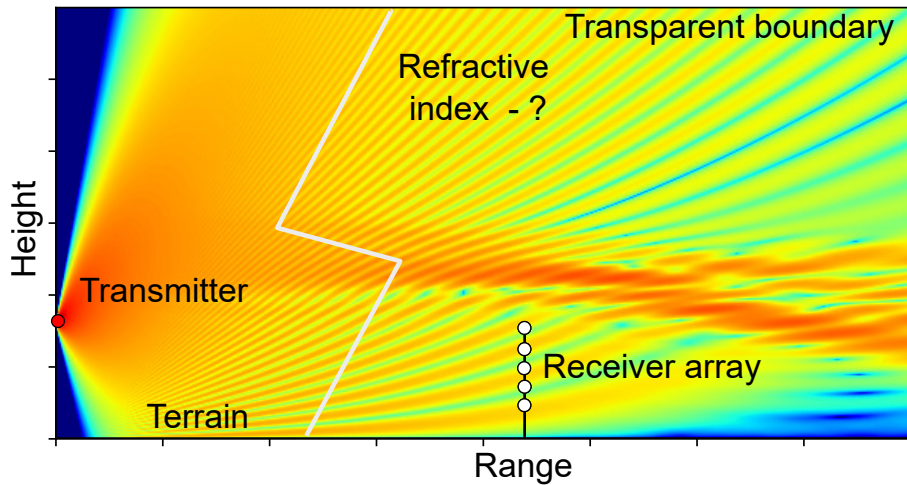


Figure 2. Tropospheric refractive index inversion. The white line indicates the (unknown) refractive index profile.

shows a pointwise comparison of the amplitudes. Although the overall qualitative and quantitative picture for the true and inverted profiles is the same, there are some local deviations that can exceed 20 dB. This should be taken into account when processing the results of real experiments.

Now let us analyze the speed and dynamics of the optimization algorithm convergence. Fig. 6 (left) shows the dependence of the minimized functional value on the iteration number of the optimization algorithm. It can be seen that the convergence does not depend significantly on the type of waveguide. The loss function decreases most rapidly up to about 100 iterations and then decreases much more slowly. Fig. 6 (right) demonstrates the dependence of the relative error between the true and inverted profiles on the iteration number. Interestingly, for the surface-based duct, the relative error continues to decrease even when the loss function values practically stop decreasing.

Next, let us analyze how the width and depth of the multilayer perceptron affect the efficiency of the proposed algorithm. Fig. 7 shows the dependence of the relative error between the true and inverted mixed profile for several different values of the depth and width of the network. It can be seen that in the single-layer case, a lower accuracy was achieved in a reasonable number of iterations than with multilayer networks. Fig. 8 demonstrates this visually. The inversion errors of the single-layer network are clearly visible, and deviations reach 10 M-units, while the multilayer network allows almost perfect inversion, even despite the noise.

A completely logical question may arise: why use neural networks if one could search for the unknown profile in the form of a simple piecewise linear or piecewise constant function, as was done in all previous works [10,27]? Fig. 9

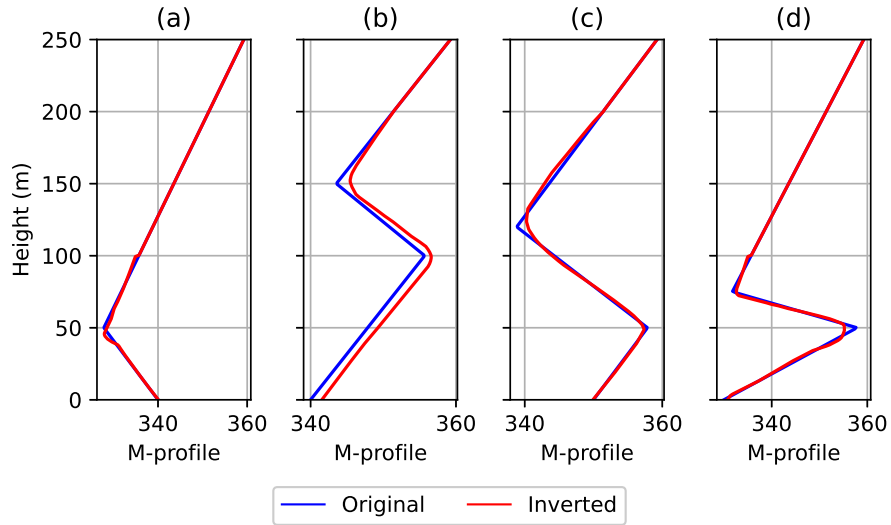


Figure 3. Original profile and inversion result. (a) Surface duct (b) Elevated duct (c) Surface-based duct (d) Combination of elevated and surface-based profiles (mixed profile).

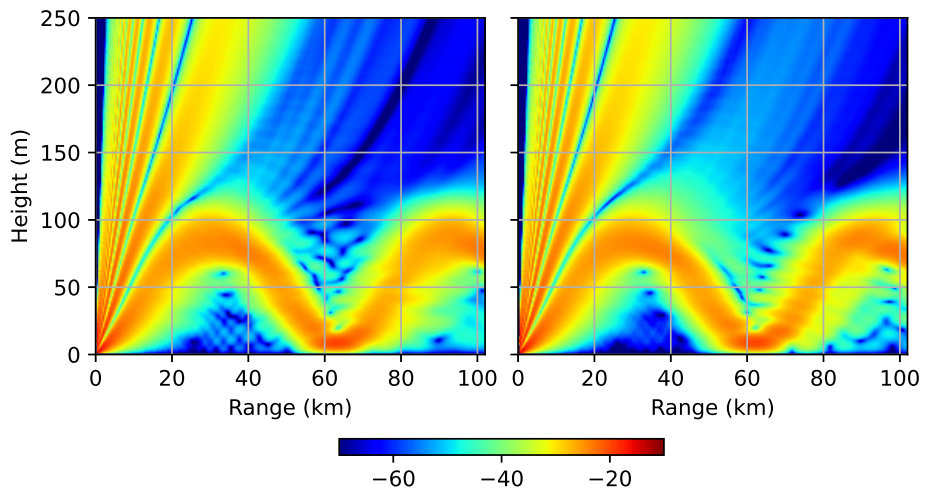


Figure 4. Distribution of the electromagnetic wave amplitude ($20 \log |\psi(x, z)|$) in the true (left) and inverted (right) surface-based ducts.

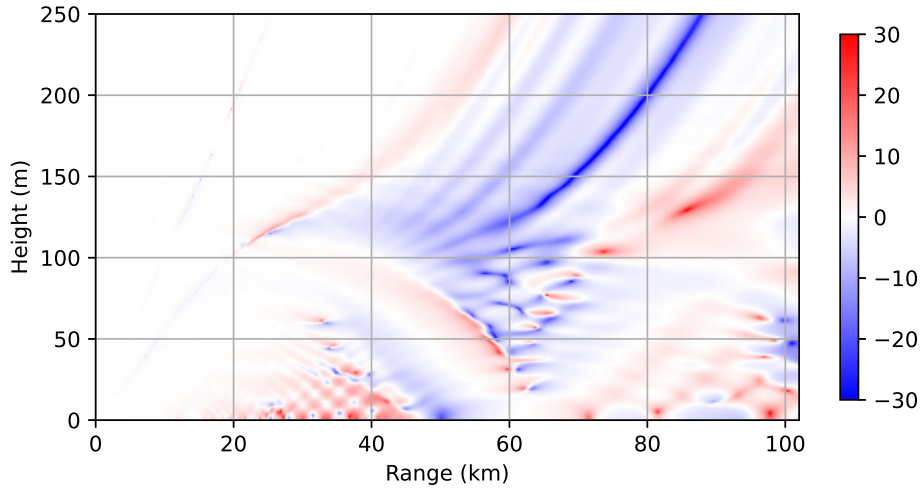


Figure 5. Difference in amplitudes between the true and inverted surface-based ducts.

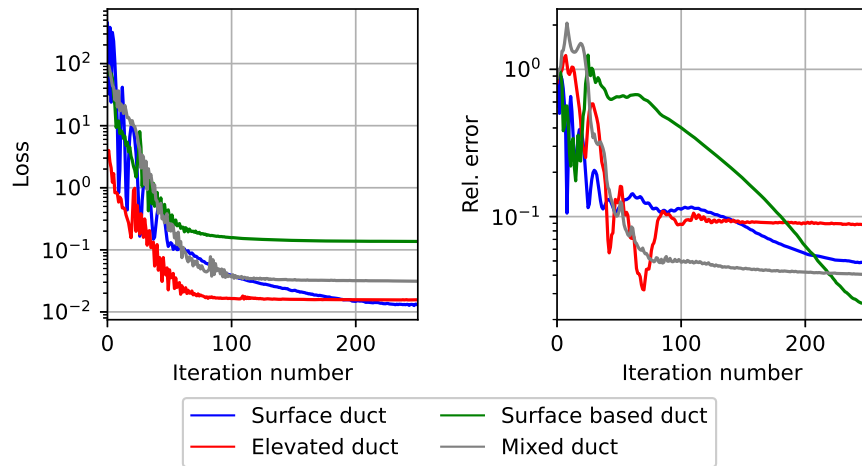


Figure 6. Dependence of the loss function value (left) and relative error (right) on the iteration number of the optimization algorithm.

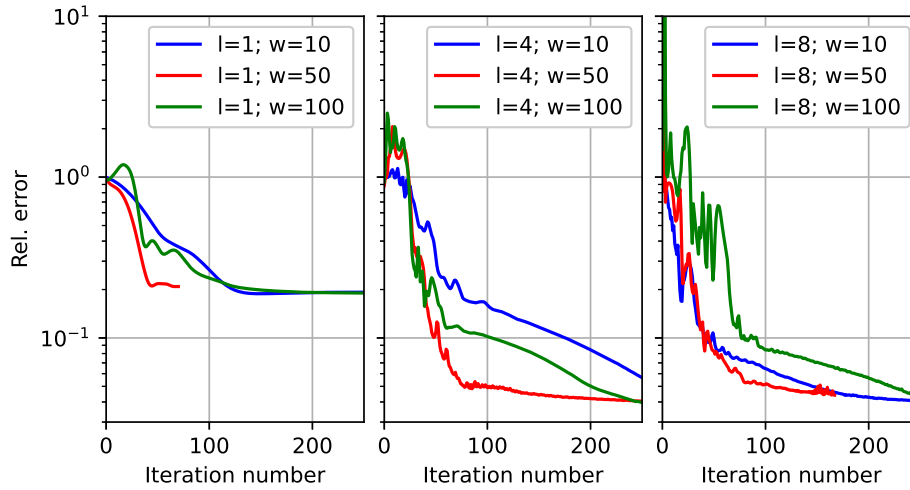


Figure 7. Dependence of the relative error between the true and inverted mixed profile for depth (l) 1, 4, and 8, and width (w) 10, 50, and 100.

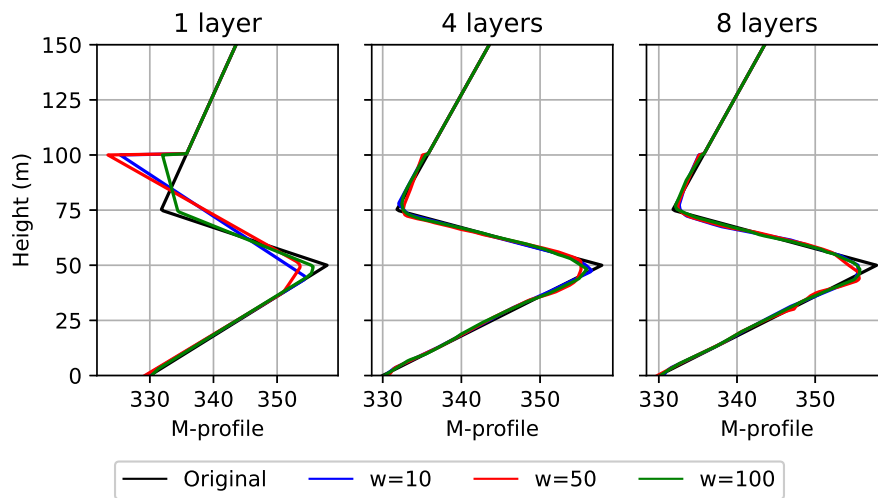


Figure 8. Original mixed profile and inversion result for various sizes of the multilayer perceptron.

shows a comparison of the convergence dynamics of the multilayer perceptron and the piecewise linear function with 50 nodes. It can be seen that the multilayer perceptron converged to the solution two orders of magnitude faster. At the same time, the found solution turned out to be closer to the true one. It should also be noted that the proposed approach allows easy use of any neural network configurations and other representations of the desired function. At the same time, changes in the method and its software implementation are minimal.

Table 1 provides a summary of the comparison of various configurations of the desired function. It can be seen that the most preferred option for the considered mixed profile was the use of a 4-layer perceptron with a layer width of 10. Single-layer models either take too long to optimize or are unable to achieve adequate accuracy. As the number of layers increases, the expressive power of the model increases, which contributes to faster and more accurate convergence to the exact solution. At the same time, excessive increase in the number of layers and network width leads only to the complication of the model and its convergence time but no longer leads to an increase in accuracy. Thus, there is some optimal network topology in terms of accuracy and convergence speed, but the question of how to quickly find it remains open.

It should be noted that previously proposed inversion methods [10,27] relied heavily on the initial approximation. In fact, they work well only when the initial approximation is close to the true value of the refractive index. The proposed method, on the other hand, does not require any prior information about the refractive index distribution, which makes this method significantly more universal.

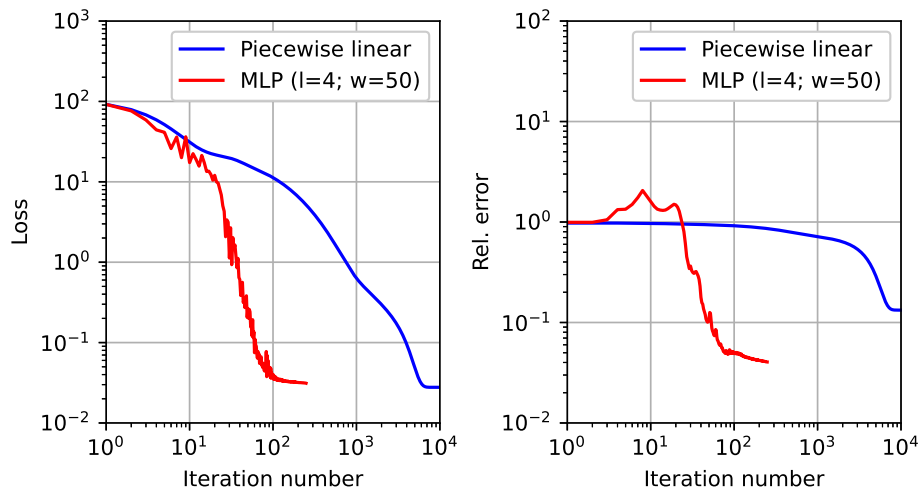


Figure 9. Dependence of the loss function value (left) and relative error (right) on the iteration number for the multilayer perceptron and the piecewise linear function.

Table 1. Convergence parameters of various refractive index models.

Method	Number of iterations	Inversion time (s)	Error
MLP (l=1, w=10)	312	59	0.188
MLP (l=1, w=50)	71	23	0.207
MLP (l=1, w=100)	1477	400	0.068
MLP (l=4, w=10)	548	168	0.022
MLP (l=4, w=50)	304	376	0.038
MLP (l=4, w=100)	384	863	0.032
MLP (l=8, w=10)	385	165	0.0373
MLP (l=8, w=50)	168	519	0.044
MLP (l=8, w=100)	456	1885	0.0298
Piecewise linear (50 points)	10000	2169	0.13

4.2 Underwater sound speed determination

A similar problem in essence and importance arises in underwater acoustics. It is required to determine the dependence of the sound speed in water on depth. The schematic description of the problem is shown in Fig. 10. An acoustic wave source is submerged underwater and emits an acoustic signal at a certain frequency. As the signal propagates from the source to the hydrophone array, it is distorted under the influence of sound speed inhomogeneities. The task is to determine the vertical sound speed profile based on the acoustic pressure measurements at the hydrophones. Although this problem has a completely different physical nature [18], it corresponds to the same mathematical model as the tropospheric inversion problem. In both problems, there is a waveguide formed by the refractive index. In both cases, wave propagation satisfies the Helmholtz equation (1).

Acoustic waveguides caused by inhomogeneous vertical stratification of sound speed can facilitate the propagation of acoustic signals over hundreds and thousands of kilometers or, conversely, contribute to their attenuation near the source. Direct measurements of sound speed are often difficult, so the problem of inversion based on indirect data is very relevant. Fig. 11 shows the inversion results for four typical sound speed profiles in shallow water. An array of 15 hydrophones was located at a distance of 3 km from the source. The signal frequency was 200 Hz. It can be seen that the proposed method successfully inverted all four considered profiles. As before, the method does not require any prior information about the desired profiles.

5 Conclusion

Unlike PINN, the proposed approach uses the existing well established numerical method for solving the direct problem, as it more reliable and efficient. That

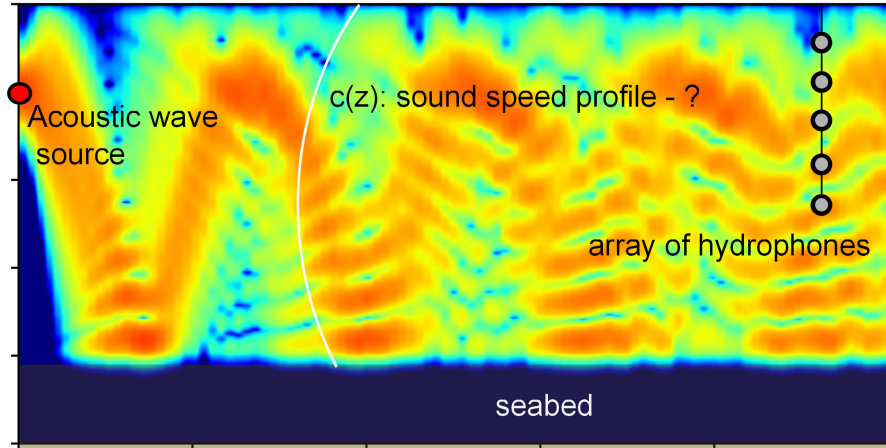


Figure 10. Schematic description of underwater sound speed inversion.

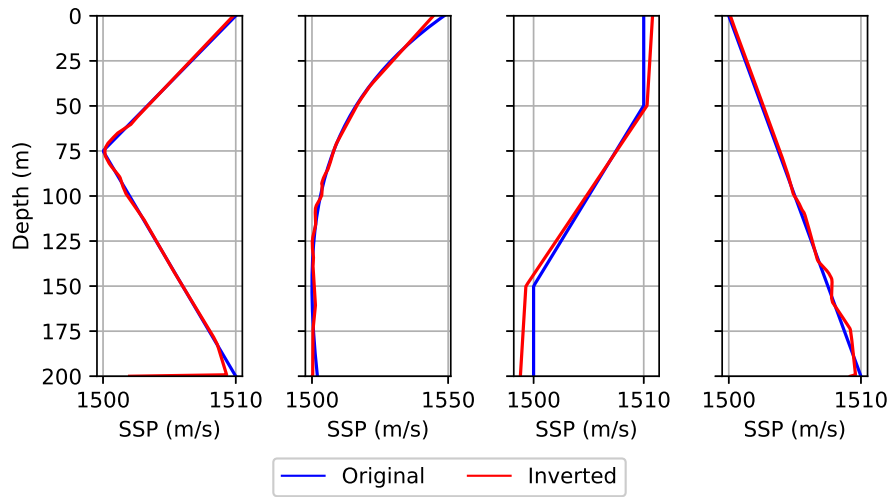


Figure 11. Original sound speed profile and inversion result.

is, the method uses not only physical laws («physics informed») but also the specifics of their numerical implementation, making it «numerical method informed». This approach seems significantly more interpretable and numerically efficient.

The use of a deep neural network as representation of the desired refraction index profile allows significantly better finding of the global minimum of the posed optimization problem. The method does not require prior information and works orders of magnitude faster than global optimization methods such as simulated annealing or genetic algorithms. Apparently, this is achieved due to the greater expressive power of the deep networks. It may seem counterintuitive that a neural network with hundreds of parameters finds a solution better than a simple piecewise linear approximation. It would seem that it should simply overfit. Nevertheless, this does not happen, and a deeper network shows better results. The theoretical aspects of this curious and useful result remain to be clarified.

Meta-parameters sometimes have to be manually tuned, which complicates the use of this method in applied problems. It will be burdensome and time-consuming for a hydroacoustic engineer or radio physicist to select the artificial parameters. Therefore, an actual direction for further research is the application of autoML [11] and the selection of the optimal neural network automatically.

Acknowledgments. This study was supported by the State research (Topic No. FFZF-2025-0006).

References

1. Ataei, M., Salehipour, H.: Xlb: A differentiable massively parallel lattice boltzmann library in python. *Computer Physics Communications* **300**, 109187 (2024)
2. Baydin, A.G., Pearlmutter, B.A., Radul, A.A., Siskind, J.M.: Automatic differentiation in machine learning: a survey. *Journal of machine learning research* **18**(153), 1–43 (2018)
3. Bezgin, D.A., Buhendwa, A.B., Adams, N.A.: Jax-fluids: A fully-differentiable high-order computational fluid dynamics solver for compressible two-phase flows. *Computer Physics Communications* **282**, 108527 (2023)
4. Chen, R.T., Rubanova, Y., Bettencourt, J., Duvenaud, D.K.: Neural ordinary differential equations. *Advances in neural information processing systems* **31** (2018)
5. Collins, M.D., Siegmund, W.L.: *Parabolic Wave Equations with Applications*. Springer (2019)
6. Colton, D., Kress, R.: *Inverse acoustic and electromagnetic scattering theory*. Springer Science & Business Media (2012)
7. Fallat, M.R., Dosso, S.E.: Geoacoustic inversion via local, global, and hybrid algorithms. *The Journal of the Acoustical Society of America* **105**(6), 3219–3230 (1999)
8. Fishman, L., McCoy, J.J.: Derivation and application of extended parabolic wave theories. i. the factorized Helmholtz equation. *J. Math. Phys.* **25**(2), 285–296 (1984)
9. Jensen, F.B., Kuperman, W.A., Porter, M.B., Schmidt, H.: *Computational ocean acoustics*. Springer Science & Business Media (2014)

10. Karabaş, U., Diouane, Y., Douvenot, R.: A variational adjoint approach on wide-angle parabolic equation for refractivity inversion. *IEEE Transactions on Antennas and Propagation* **69**(8), 4861–4870 (2021)
11. Karmaker, S.K., Hassan, M.M., Smith, M.J., Xu, L., Zhai, C., Veeramachaneni, K.: Automl to date and beyond: Challenges and opportunities. *ACM Computing Surveys (CSUR)* **54**(8), 1–36 (2021)
12. Kidger, P., Foster, J., Li, X.C., Lyons, T.: Efficient and accurate gradients for neural sdes. *Advances in Neural Information Processing Systems* **34**, 18747–18761 (2021)
13. Kingma, D.P.: Adam: A method for stochastic optimization. arXiv preprint arXiv:1412.6980 (2014)
14. Levy, M.F.: *Parabolic Equation Methods for Electromagnetic Wave Propagation*. The Institution of Electrical Engineers, UK (2000)
15. Lu, L., Meng, X., Mao, Z., Karniadakis, G.E.: DeepXDE: A deep learning library for solving differential equations. *SIAM Review* **63**(1), 208–228 (2021)
16. Lytaev, M.S.: *PyWaveProp* (2024), <https://github.com/mikelytaev/wave-propagation>
17. Lytaev, M.: Automatically differentiable higher-order parabolic equation for real-time underwater sound speed profile sensing. *Journal of Marine Science and Engineering* **12**(11), 1925 (2024)
18. Lytaev, M.S.: Rational interpolation of the one-way Helmholtz propagator. *J. Comput. Sci.* p. 101536 (2022)
19. Papadakis, J.S., Karasmani, E.: Gradient of the cost function via the adjoint method for underwater acoustic inversion. *Journal of Theoretical and Computational Acoustics* **28**(01), 1950010 (2020)
20. Pastore, D.M., Greenway, D.P., Stanek, M.J., Wessinger, S.E., Haack, T., Wang, Q., Hackett, E.E.: Comparison of atmospheric refractivity estimation methods and their influence on radar propagation predictions. *Radio Science* **56**(9), 1–17 (2021)
21. Pastore, D.M., Wessinger, S.E., Greenway, D.P., Stanek, M.J., Burkholder, R.J., Haack, T., Wang, Q., Hackett, E.E.: Refractivity inversions from point-to-point x-band radar propagation measurements. *Radio Science* **57**(2), 1–16 (2022)
22. Sapunov, G.: *Deep Learning with JAX*. Manning (2024)
23. Sen, M.K., Stoffa, P.L.: *Global optimization methods in geophysical inversion*. Cambridge University Press (2013)
24. Thiyagalingam, J., Shankar, M., Fox, G., Hey, T.: Scientific machine learning benchmarks. *Nature Reviews Physics* **4**(6), 413–420 (2022)
25. Tichonov, A.N., Leonov, A.S., Jagola, A.G.: *Nonlinear ill-posed problems*, vol. 1. Chapman & Hall London (1998)
26. Xue, T., Liao, S., Gan, Z., Park, C., Xie, X., Liu, W.K., Cao, J.: Jax-fem: A differentiable gpu-accelerated 3d finite element solver for automatic inverse design and mechanistic data science. *Computer Physics Communications* **291**, 108802 (2023)
27. Zhao, X., Wang, D.: Ocean acoustic tomography from different receiver geometries using the adjoint method. *The Journal of the Acoustical Society of America* **138**(6), 3733–3741 (2015)